AD-A264 334

TATION PAGE

1. AGENCY USE ONLY (Leave blank)	IT DATE	3. REPORT TYPE AND DATES COVERED
		Final Report 15 Nov 88-31 Dec 92

4. TITLE AND SUBTITLE	5. FUNDING NUMBERS
Fundamental studies of the mechanical behavior of microelectronics thin film materials	AFOSR-89-0185

6. AUTHOR(S)

Professor William D. Nix

7. PERFORMING ORGANIZATION NAME(S) AND ADDRESS(ES)	8. PERFORMING ORGANIZATION REPORT NUMBER
Department of Materials Sciences & Engineering Stanford University Stanford CA 94305	AFOSR-TR. 9 3 0 0 7 2

9. SPONSORING / MONITORING AGENCY NAME(S) AND ADDRESS(ES)	10. SPONSORING / MONITORING AGENCY REPORT NUMBER
AFOSR NE 110 Duncan Avenue Suite B115 Bolling AFB DC 20332-0001	2305/C1

DTIC ELECTE MAY 1 4 1993 S D C

11. SUPPLEMENTARY NOTES

12a. DISTRIBUTION / AVAILABILITY STATEMENT	12b. DISTRIBUTION CODE
UNLIMITED	

13. ABSTRACT (Maximum 200 words) This document represents a final technical report for AFOSR Grant No. 89-0185. The research program supported under this grant involved a fundamental study of the mechanical properties of microelectronic thin film materials. The focus of the work was on the microscopic processes that lead to stresses in microelectronic thin films and control the mechanical properties of these materials. Our work ranged form studies of interconnect metals, passivation glasses and heteroepitaxial thin film semiconductors. In previous reports we highlighted work done of the mechanical properties of passivation glasses and interconnect metals and the processes of failure of interconnect metals. In this final report we highlighted our work on misfit dislocation formation in hetero-pitaxial thin films. The body of the report contains two reports of our work on misfit dislocations. Our overall understanding of misfit dislocations in Si-Ge layers is described in the first report. That report also descirbes our work on the effect of capping layers on the formation of misfit dislocations. The second report descirbes our in situ studies of the kinetics of formation of misfit dislocations in Si-Ge films. By measureing the change of substrates curvature as a

14. SUBJECT TERMS	15. NUMBER OF PAGES
	16. PRICE CODE

93-10671

17. SECURITY CLASSIFICATION OF REPORT	18. S O		ATION	20. LIMITATION OF ABSTRACT

function of time during annealing we were able to determine the way in which mobile threading dislocation density changes during the course of annealing. This work has led to a much more complete understanding of the kinetics of strain relaxation in heteropitaxial thin films.

The presentations and publications that have resulted from this work are listed at the end of this report.

Final Technical Report

for

AFOSR Grant No. 89-0185

FUNDAMENTAL STUDIES OF THE MECHANICAL BEHAVIOR OF MICROELECTRONIC THIN FILM MATERIALS

Submitted to :

Department of the Air Force

Directorate of Electronic and Materials Sciences

Air Force of Office of Scientific Research

Bolling Air Force Base, Building 410

Washington D.C. 20332

Attention: Dr. Gerald Witt

Submitted by:

Professor William D. Nix, Principal Investigator

Department of Materials Science and Engineering

Stanford University, Stanford, CA 94305

April 1993

Table of Contents

I. SUMMARY

This document represents a final technical report for AFOSR Grant No. 89-01185. The research program supported under this grant involved a fundamental study of the mechanical properties of microelectronic thin film materials. The focus of the work was on the microscopic processes that lead to stresses in microelectronic thin films and control the mechanical properties of these materials. Our work ranged from studies of interconnect metals, passivation glasses and heteroepitaxial thin film semiconductors. In previous reports we highlighted work done of the mechanical properties of passivation glasses and interconnect metals and the processes of failure of interconnect metals. In this final report we highlight our work on misfit dislocation formation in heteroepitaxial thin films

The body of this report contains two reports of our work on misfit dislocations. Our overall understanding of misfit dislocations in Si-Ge layers is described in the first report. That report also describes our work on the effect of capping layers on the formation of misfit dislocations. The second report describes our in situ studies of the kinetics of formation of misfit dislocations in Si-Ge films. By measuring the change of substrate curvature as a function of time during annealing we were able to determine the way in which mobile threading dislocation density changes during the course of annealing. This work has led to a much more complete understanding of the kinetics of strain relaxation in heteroepitaxial thin films.

The presentations and publications that have resulted from this work are listed at the end of this report.

II.   RESEARCH REPORT

A.   Mechanisms and Kinetics of Misfit Dislocation Formation in Heteroepitaxial Thin Films

W.D. Nix, D.B. Noble and J.F. Turlo

1.   Introduction

A great amount of attention has been focussed recently on the processes by which misfit dislocations form in heteroepitaxial structures; see, for example, [1-2]. A number of semiconductor device applications rely on the elastic strain in heteroepitaxial films to control the bandgap in these materials [3-4]. For these applications strain relaxation by misfit dislocation formation must be avoided. For other applications it may be possible to grow dislocation free, single crystal films of difficult-to-grow semiconductors through epitaxial growth on dislocation free substrates such as Si [5]. Again, misfit dislocations must be avoided. Here we review the thermodynamics, kinetics and mechanisms of misfit dislocation formation, paying particular attention to the mechanism by which a misfit dislocation forms through the incremental movement of a "threading" dislocation. This same mechanism is used to examine the effects of an unstrained capping layer on the velocity of a dislocation in a strained film. We find that the effects of an unstrained capping layer on the dislocation velocity are too small to account for the observed inhibition of misfit dislocation formation in Si-Ge films with Si capping layers. This result leads us to conclude that the primary effects of such capping layers are to inhibit dislocation nucleation and multiplication.

2.   The Critical Thickness for Misfit Dislocation Formation

Through the pioneering work of van der Merwe [6] and Matthews [7-9] it is now well established that misfit dislocations can form in heteroepitaxial films only if the film exceeds a critical thickness. Here we give a brief account of the equilibrium theory of misfit dislocations; a more complete treatment of this can be found in a recent review paper by Nix [10]. Consider a film with an equilibrium lattice parameter a_{film} deposited onto a substrate with a lattice parameter $a_{substrate}$ ($a_{substrate} < a_{film}$ for the Si-Ge system discussed in this paper). Because of the lattice mismatch, the film must be strained in order to establish an epitaxial relationship with the substrate. It is now well established that if the film is very thin, less that the critical thickness, the stable equilibrium state is one in which the film is homogeneously strained and contains no misfit dislocations. Only if the critical thickness is exceeded can the free energy of the film be reduced by the presence of

misfit dislocations. For such thicker films, introduction of misfit dislocations lowers the free energy by reducing the homogeneous elastic strain in the film. The equilibrium state can be determined by finding the misfit dislocation spacing at which this
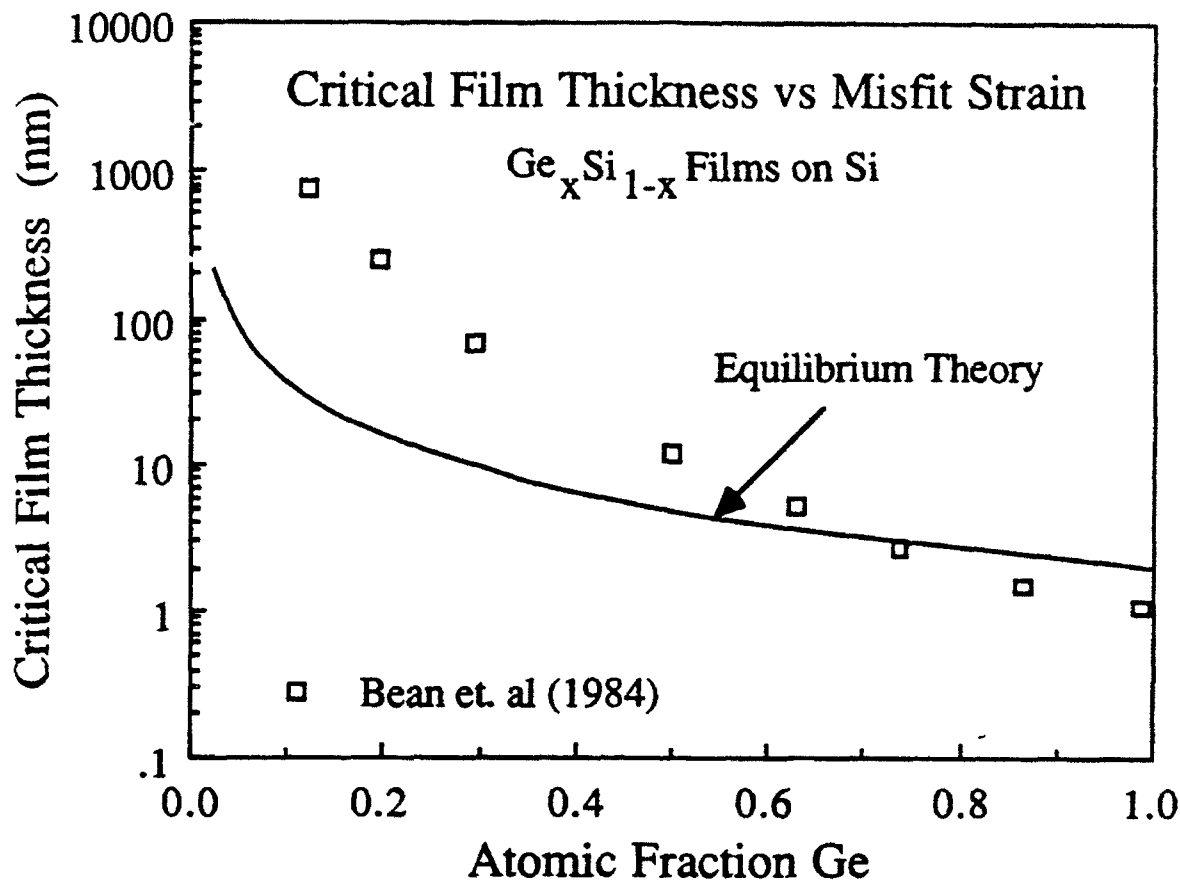
Fig. 1.   Critical film thickness versus misfit strain for Si-Ge films on Si. The results of Bean et al. [11] are compared with the equilibrium theory.

reduction in free energy is just balanced by the increase in free energy associated with the energies of the misfit dislocations themselves. Then, the critical thickness, h_c, is that film thickness for which the equilibrium misfit dislocation spacing approaches infinity. The resulting expression for the critical thickness takes the form

$$\frac{h_c}{\ln\left(\frac{\beta h_c}{b}\right)} = \frac{\mu b}{4\pi(1-\nu)M_f \varepsilon} \quad , \tag{1}$$

2

where μ and ν are isotropic elastic constants, b is the Burgers vector of the misfit dislocation, M_f is the biaxial elastic modulus of the film, B is a constant and ε is the misfit strain, defined in the present discussion to be

$$\varepsilon = \frac{a_{film} - a_{substrate}}{a_{substrate}} \approx \frac{a_{film} - a_{substrate}}{a_{film}} \qquad (?)$$
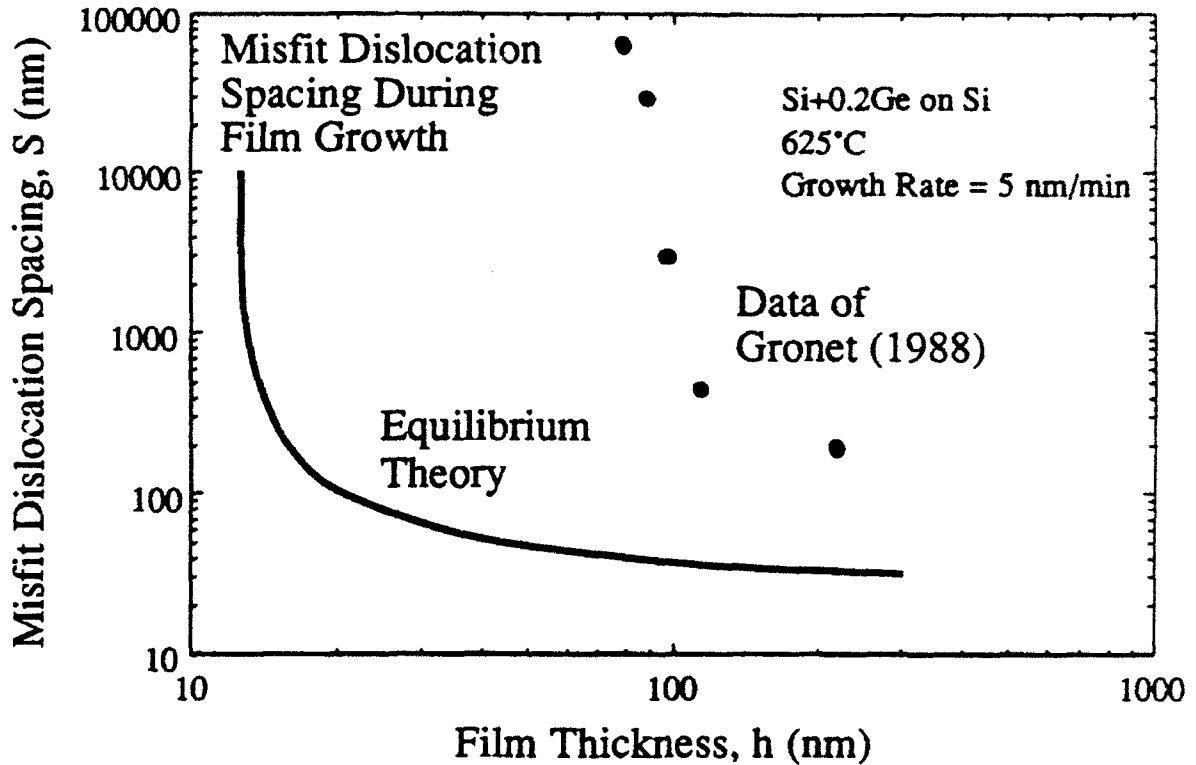
Fig. 2.   Misfit dislocation spacing in Si-Ge films grown to various thicknesses on Si [1]. The observed dislocation spacings are compared with the predictions of the equilibrium theory.

The equilibrium model shows that the critical thickness depends strongly on the misfit strain ε. For Si-Ge films on Si substrates, the misfit strain varies almost linearly with the atomic fraction of Ge in the film. As a result, the predicted critical thickness depends on the composition of the film, as shown in Fig. 1. The figure also includes experimental measurements of the critical thickness reported by Bean et.al..[11]. We note that for films containing between 15 and 30 atomic percent Ge, the actual film thicknesses at which misfit dislocations are first observed are much greater that

3

the critical thicknesses predicted by the equilibrium theory. This same discrepancy is also shown in Fig. 2, where the misfit dislocation spacings predicted by the equilibrium theory are compared with observed misfit dislocation spacings for Si-Ge films grown on Si. These data were obtained for Si + 0.2Ge films grown on Si by limited reaction processing [1]. We note that the observed misfit dislocation spacings are very much greater than the predictions of the equilibrium theory, especially below a film thickness of about 80 nm. This apparent critical thickness is very much greater than the critical thickness of 13.5 nm predicted by the equilibrium theory. We believe the discrepancies shown in these figures are due to the sluggishness of the processes by which misfit dislocations form. The kinetic factors responsible for these effects are described in the next section.

3. Kinetic Theory of Misfit Dislocation Formation

The Dislocation Velocity

The kinetics of forming misfit dislocations can be studied by considering the mechanism by which a misfit dislocation forms. Following the work of Matthews [7-9], we consider that misfit dislocations are created by the movement of "threading" dislocations that deposit misfit dislocations at the film/substrate interface as they move. We use the quotation marks here and throughout this paper to denote any dislocation that extends from the film/substrate interface to the free surface of the film; the "threading" dislocation need not have originated in the substrate. Figure 3 shows a "threading" dislocation moving in a film and depositing a misfit dislocation as it moves. The kinetics of movement of the dislocation can be studied by using the methods of Matthews [7-9] and Freund [12-13], who showed that the work done on the moving dislocation by the stress in the film must be greater that the work needed to form the misfit dislocation. For the case of a Si-Ge film grown onto a (001) Si substrate, the work done by the stress in the film for a unit displacement of the "threading" dislocation is

$$W_{layer} = \sqrt{\frac{3}{2}}\,\tau bh = \frac{\sigma bh}{2} \quad , \tag{3}$$

where τ is the resolved shear stress and σ the biaxial stress in the film, b is the Burgers vector, h is the film thickness and the numerical factors reflect the orientation of the slip plane and slip direction in the (001) film. For the (001) film under consideration, the misfit dislocation is a 60 degree mixed dislocation. The energy of a unit length of such a misfit dislocation is

4

$$W_{60\,deg} = 0.95 \frac{b^2}{4\pi(1-\nu)} \frac{2\mu_f\mu_s}{(\mu_f + \mu_s)} \ln\left(\frac{\beta h}{b}\right) \quad , \tag{4}$$

where μ_f and μ_s are the shear moduli of the film and substrate, respectively, β is a constant taken to be 0.755 and the other terms have their usual meaning [10]. Freund [12-13] has shown that
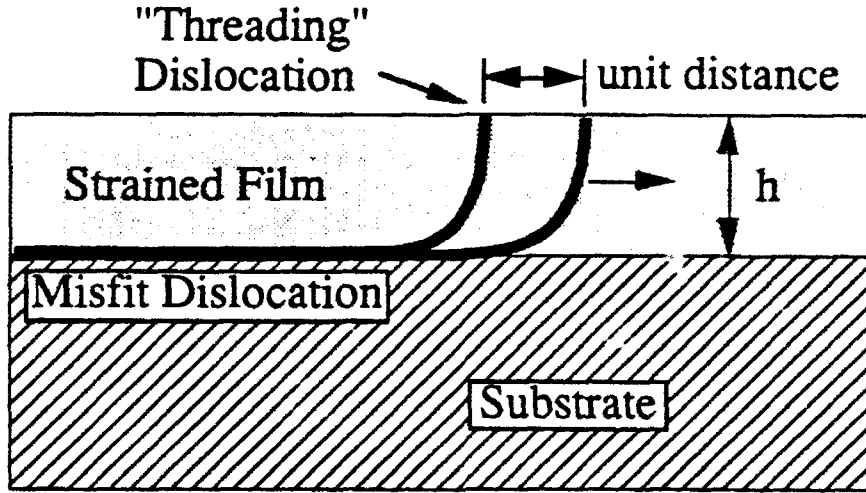

Fig. 3.   Motion of a "threading" dislocation which produces a misfit dislocation at the interface between the strained film and the substrate. Movement of the "threading" dislocation by a unit distance creates a unit length of misfit dislocation.

the critical film thickness can be derived by setting $W_{layer} = W_{60deg}$. This is a condition of equilibrium, at which point the "threading" dislocation does not move. For the "threading" dislocation to move at a finite velocity and to deposit a misfit dislocation as it moves, W_{layer} must be greater that W_{60deg}. We define $W_{net} = W_{layer} - W_{60deg}$ as the net work done on the moving dislocation as it moves a unit distance. We may think of this net work as being done by an effective shear stress defined by

$$\tau_{eff}\, bh\sqrt{\frac{3}{2}} = W_{net} = W_{layer} - W_{60\,deg} \quad , \tag{5}$$

This effective stress drives the "threading" dislocation at a finite velocity, and leads to the dissipation of the net work as heat. Using eqns. (3) and (4) the effective shear stress may be written in final form as

$$\tau_{eff} = \tau - 0.95 \sqrt{\frac{2}{3}} \frac{b}{4\pi(1-v)} \frac{2\mu_f \mu_s}{(\mu_f + \mu_s)} \frac{1}{h} \ln\left(\frac{\beta h}{b}\right) \quad , \tag{6}$$

$$\tau_{eff} = \tau - A \frac{1}{h} \ln\left(\frac{\beta h}{b}\right) \quad , \tag{7}$$

or

$$\tau_{eff} = \tau - \tau_{threshold} \quad . \tag{8}$$

Hereafter, we use the symbol A to describe the coefficient of the logarithmic term:

$$A = 0.95 \sqrt{\frac{2}{3}} \frac{b}{4\pi(1-v)} \frac{2\mu_f \mu_s}{(\mu_f + \mu_s)} \quad , \tag{9}$$

because it appears in so many of the equations. We note that the critical thickness can be found by setting $\tau_{eff} = 0$. For the "threading" dislocation to move at a finite velocity the effective shear stress must be greater than zero, $\tau_{eff} > 0$.

The effective shear stress developed here is equivalent to the "excess" stress discussed by Dodson and Tsao [14-15]. It is that part of the shear stress which is not balanced by the drag of the misfit dislocation and is available to drive the "threading" dislocation forward. We use the effective stress terminology here because it is well established in the literature on creep of diamond cubic crystals [16].

The rate of motion of the "threading" dislocation in the Si-Ge film is assumed to be governed by the thermally activated nucleation and motion of kinks along the dislocation line. Because these are near-atomic scale processes, it is expected that the kinetics of dislocation motion in thin film structures will be the same as for bulk crystals. Accordingly, based on experimental work of Alexander and Haasen [17], we assume that the "threading" dislocation velocity can be expressed as

$$v = B \exp\left(-\frac{U}{kT}\right)\left(\frac{\tau_{eff}}{\tau_o}\right)^{1.2} \quad , \tag{10}$$

6

where U is the activation energy for dislocation motion, B (= 7.33×10^4 m/s) and τ_0 (=9.8Mpa) are constants and τ_{eff} is the effective stress for dislocation motion given by eqn. (6). Activation energies for dislocation motion in Si and Ge were measured by Alexander and Haasen using etch pitting methods. Their results are shown in Table I. Also shown in Table I are activation energies for dislocation motion in Si-Ge films, reported recently by Hull et al.. [18] and Tuppen and Gibbings [19]. The results of Hull et al..[18] are based on in-situ annealing of TEM samples whereas the results of Tuppen and Gibbings [19] are based on a scratch/etching method. The results of Hull et al..[18] suggest that the activation energy might depend strongly on composition or strain. We have also conducted in-situ TEM annealing experiments on Si$_{1-x}$Ge$_x$ films with the following compositions: x = 0.16, 0.22, 0.34. We find the activation energy for motion to be 2.2 $\pm$ 0.2 eV for all compositions (and strains) studied. Some of these experimental results are shown in Fig. 4.

Table I
Reported Activation Energies for Dislocation Motion in Si, Ge and Si-Ge Epitaxial Thin Films

Material	Technique	Activation Energy	Reference
Bulk Si	Etch Pitting	2.2 eV	Alexander and Haasen [17]
Bulk Ge	Etch Pitting	1.6 eV	Alexander and Haasen [17]
Strained Si$_{1-x}$Ge$_x$ Layers (x=0.3)	In-Situ TEM Annealing	1.1$\pm$0.2 eV	Hull et al . [18]
Strained Si$_{1-x}$Ge$_x$ Layers (x=0.05,0.13)	Scratch/ Etching	2.2$\pm$0.2 eV	Tuppen and Gibbings [19]
Strained Si$_{1-x}$Ge$_x$ Layers (x=0.16,0.22,0.34)	In-Situ TEM Annealing	2.2$\pm$0.2 eV	present work

A few comments should be made about the discrepancy that exists between the results of Hull et al. [18] and the present work. Two different observational techniques have been used to determine

7

the activation energies for dislocation motion in the in-situ TEM annealing experiments. The technique used by Hull et al.. [18], and also in preliminary experiments in the present work, involves the observation of a particular area of the foil and the measurement of the velocities of the dislocations that happen to come into view. We found an activation energy of 1.3-1.6 eV for a film with 22% Ge using this technique. A different technique was used to obtain the experimental data shown in Fig. 4. In this method a suitable dislocation is found when the temperature is low and its motion is monitored as the sample is heated to progressively higher temperatures. Because dislocation velocities are so fast at high temperatures the individual dislocation measurements could be carried out only in the range of 520-675°C. Higher temperature measurements were taken from randomly captured events. This method gives an activation energy of 2.2 eV, even for a film with 30% Ge.

The technique based on the observation of a particular area of the foil may give erroneous activation energies because at lower temperatures only the fastest dislocations are observed, whereas at high temperatures all dislocations in the velocity spectrum may be sampled. This could produce the low apparent activation energies that have been observed.

Because the single dislocation in-situ TEM annealing experiments give results that are in agreement with the etch pitting results of Tuppen and Gibbings [19] and Alexander and Haasen [17], we conclude that the activation energy for motion of "threading" dislocations in Si-Ge films is about 2.2 eV.

Evolution of the Misfit Dislocation Density

We may now calculate the rate at which misfit dislocations are formed in an epitaxial Si-Ge film with a fixed density, N, of "threading" dislocations. Because each "threading" dislocation creates a misfit dislocation as it moves, it follows that the mean spacing, S, between misfit dislocations changes with time according to

$$\frac{d\left(\frac{1}{S}\right)}{dt} = \frac{Nv}{2} \quad , \tag{11}$$
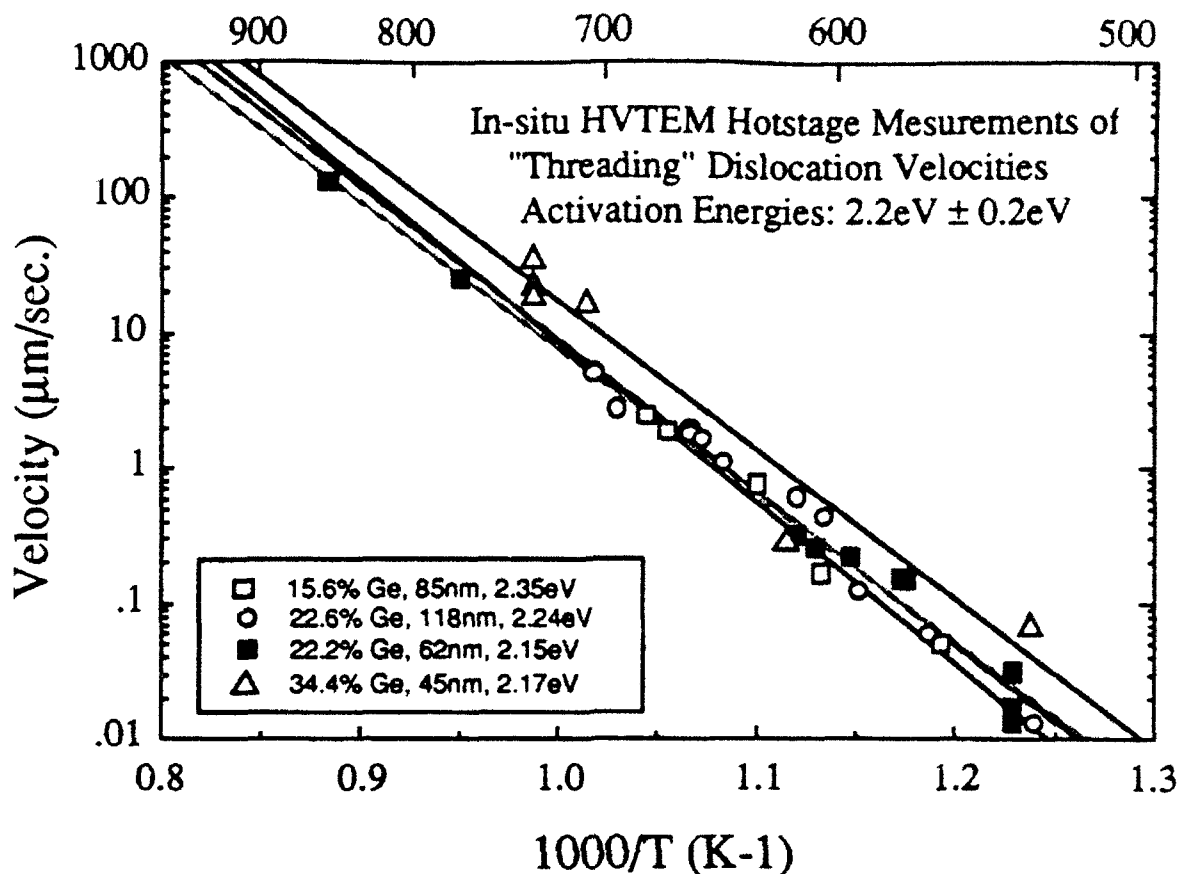
8

Fig. 4. In-Situ high voltage TEM measurements of "threading" dislocation velocities in Si-Ge films. Measurements are based on the technique of measuring the motion of an individual dislocation at various temperatures. The measured activation energy is 2.2 eV.

where v is the "threading" dislocation velocity given by eqn. (10). These equations can be used to predict the evolution of the misfit dislocation spacing during film growth. Results for different "threading" dislocation densities are shown in Fig. 5 and compared with equilibrium predictions. We note that for a low "threading"dislocation density the predicted misfit dislocation spacings are much larger than the equilibrium spacings. However, these predictions for a constant "threading" dislocation density are unlike the data shown in Fig. 2. A rapid reduction in the misfit dislocation spacing at a film thickness of about 80 nm is not predicted. We believe that this rapid change in the misfit dislocation spacing is caused by the nucleation of new "threading" dislocations and the multiplication of existing ones.

9

Following methods developed in the creep literature [16] we may assume that "threading" dislocations multiply according to a law of the form

$$\left(\frac{dN}{dt}\right)_{multiplication} = N\delta v \quad , \tag{12}$$

where δ is a breeding factor. When this law is used in conjunction with eqn. (11) the misfit dislocation spacing is predicted to change more abruptly during film growth. Results for various constant breeding factors are shown in Fig. 6. We note that a sharp reduction in the misfit dislocation spacing is predicted to occur near a film thickness of 100nm.
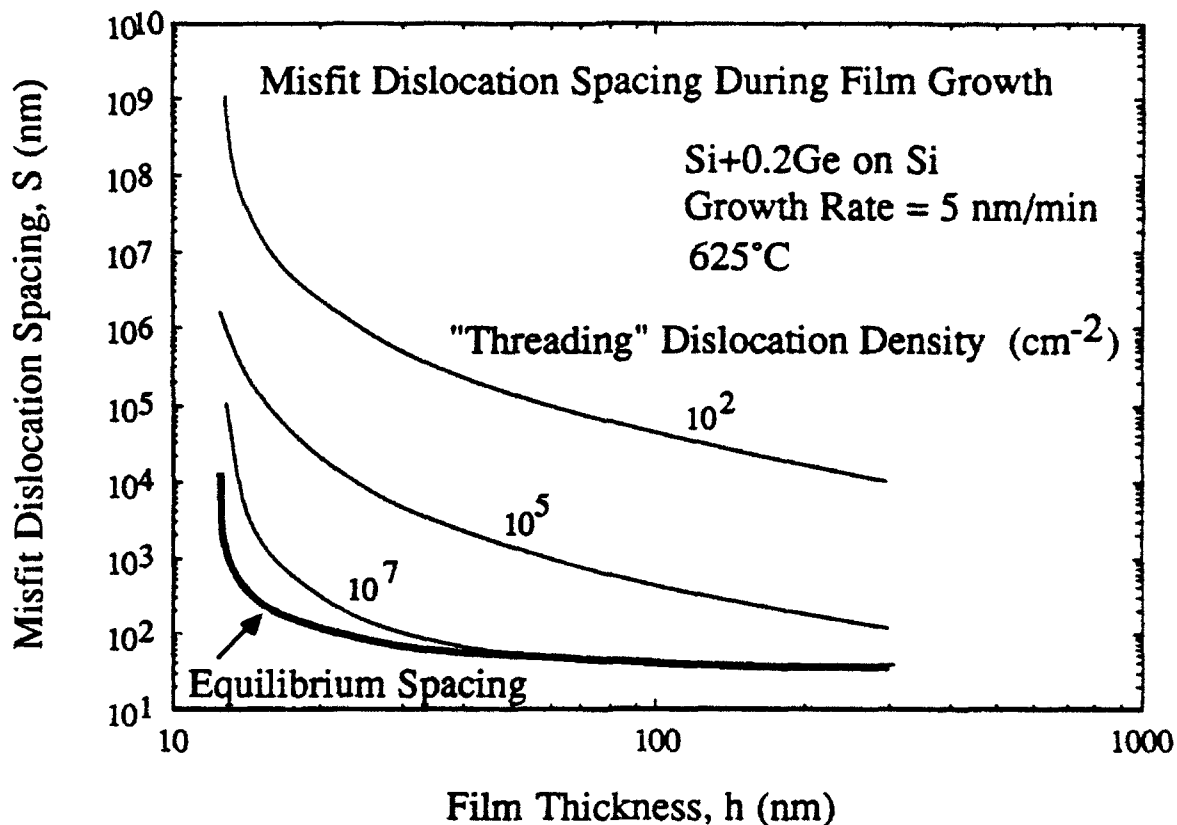

Fig. 5.   Computed misfit dislocation spacings during the growth of a Si-Ge film on Si for different constant "threading" dislocation densities. The results are compared with the predictions of the equilibrium theory.
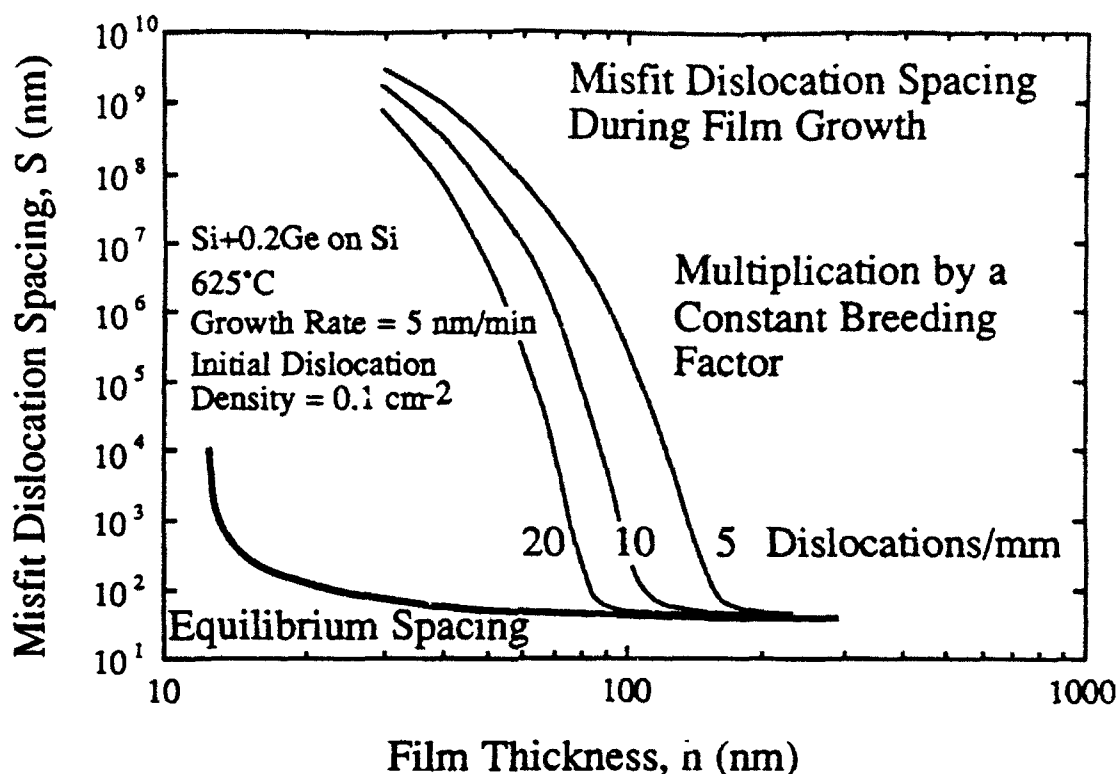
Fig. 6. Computed misfit dislocation spacings during the growth of a Si-Ge film on Si for various constant breeding factors.. The results are compared with the predictions of the equilibrium theory.

It is now well established that misfit dislocations can form during high temperature annealing of films that were initially dislocation free. This indicates strongly that dislocation nucleation, which probably occurs at the free surface of the film, also contributes significantly to the formation of new "threading" dislocations. Such dislocation nucleation, although not well understood, is expected to cause the misfit dislocation spacing to decrease abruptly with increasing film thickness.

Kinetics of Strain Relaxation

The processes of misfit dislocation formation discussed here lead to a relaxation of the homogeneous elastic strain in the film. This relaxation may be expressed as a biaxial plastic strain rate of the form

$$\dot{\epsilon}_{plastic} = \frac{1}{4} Nbv \quad , \tag{13}$$

or a stress relaxation rate of the form

$$\frac{d\sigma}{dt} = - M_f \dot{\epsilon}_{plastic} \quad . \tag{14}$$

These equations can be used to describe the kinetics of strain relaxation at elevated temperatures, provided they are coupled with an equation for the evolution of the "threading" dislocation density. Assuming that both nucleation and multiplication of "threading" dislocations occurs, an evolutionary equation of the form

$$\frac{dN}{dt} = \left(\frac{dN}{dt}\right)_{nucleation} + N\delta v \quad , \tag{15}$$

can be used.

4.   Effects of Unstrained Capping Layers on the Processes of Misfit Dislocation Formation

Unstrained epitaxial capping layers on strained epitaxial films are a natural feature of some device structures. Such layers are known to inhibit the formation of misfit dislocations within the strained film. Here we consider the physical processes by which the formation of misfit dislocations might be inhibited.

Effects of Unstrained Capping Layers on the Motion of "Threading" Dislocations

Here we consider the influence of unstrained capping layers on the motion of "threading" dislocations in strained films. In each of the cases to be discussed, an effective shear stress for dislocation motion will be determined. These effective stresses will lead directly to predicted velocities through the use of eqn. (10).

We consider first an unstrained capping layer which is sufficiently thin that the "threading" dislocation is able to drag through the cap as it moves. This is depicted in Fig. 7. Because the capping layer has the same lattice parameter as the substrate, it is not elastically strained and it does not exert forces on the part of the "threading" dislocation that lies in the capping layer. As a consequence, the part of the "threading" dislocation that extends through the capping layer must be dragged along by the part of the dislocation that lies in the strained film. As shown in the figure, forces can be transmitted to the dislocation segment in the unstrained capping layer through line tension effects. The effective stress for dislocation motion in such a capped structure can be expressed as

$$\tau_{eff}^{cut} = \tau\left(\frac{h}{h+t}\right) - A\left\{\frac{1}{(h+t)}\ln\left(\frac{\beta(h+t)}{b}\right)\right\} \quad , \qquad (16)$$

where the notation "cut" signifies that the "threading" dislocation cuts through the cap, t is the thickness of the capping layer and the other terms are the same as those defined for eqn. (6). This equation differs for eqn.(6) in two ways. First, the logarithmic term includes the total thickness of the strained film and the capping layer, h+t, because the "threading" dislocation moves through both layers. Second, the term involving the shear stress τ is reduced by the fraction h/(h+t) to reflect the fact that work is done only on that part of the "threading" dislocation that lies in the strained film.

If the thickness of the capping layer is greater than a critical thickness, then the moving dislocation does not cut through the cap and is confined to move within the strained film. This is illustrated in Fig. 8. For this case, two dislocations are left behind the moving dislocation, one at the film/substrate interface and one at the interface between the film and the capping layer. In this case the effective shear stress for dislocation motion is defined in terms of the work done on the moving dislocation by the stress in the film, less the work needed to form the two misfit dislocations:

$$\tau_{eff}^{dipole} = \tau - A\left\{\frac{1}{h}\ln\left(\frac{\sqrt{3}\,\beta h}{2\sqrt{2}\,b}\right)\right\} - A\left\{\frac{1}{h}\ln\left(\frac{\sqrt{3}\,\beta h}{2\sqrt{2}\,b}\right)\right\} \quad . \qquad (17)$$

The two identical logarithmic terms are associated with the energies of the two misfit dislocations. The numerical factors in the argument of the logarithmic terms are needed to compute the cut off radii for the two dislocations in the dipole.

13
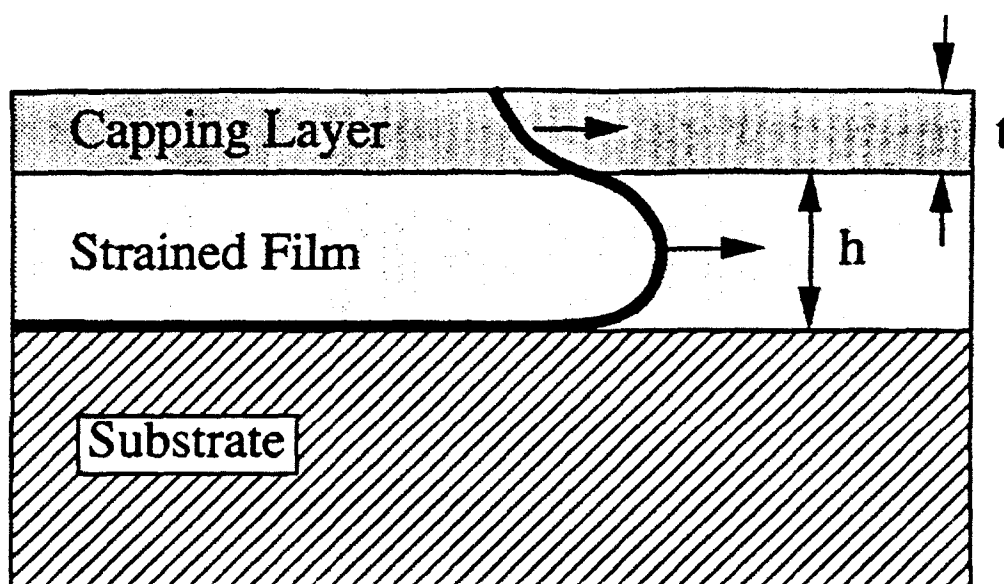
Fig. 7.　Motion of a "threading" dislocation that cuts through a thin capping layer. The capping layer is, like the substrate, unstrained. Forces on the segment that extends through the capping layer are provided by line tension effects. The velocity of the dislocation is v(cut).
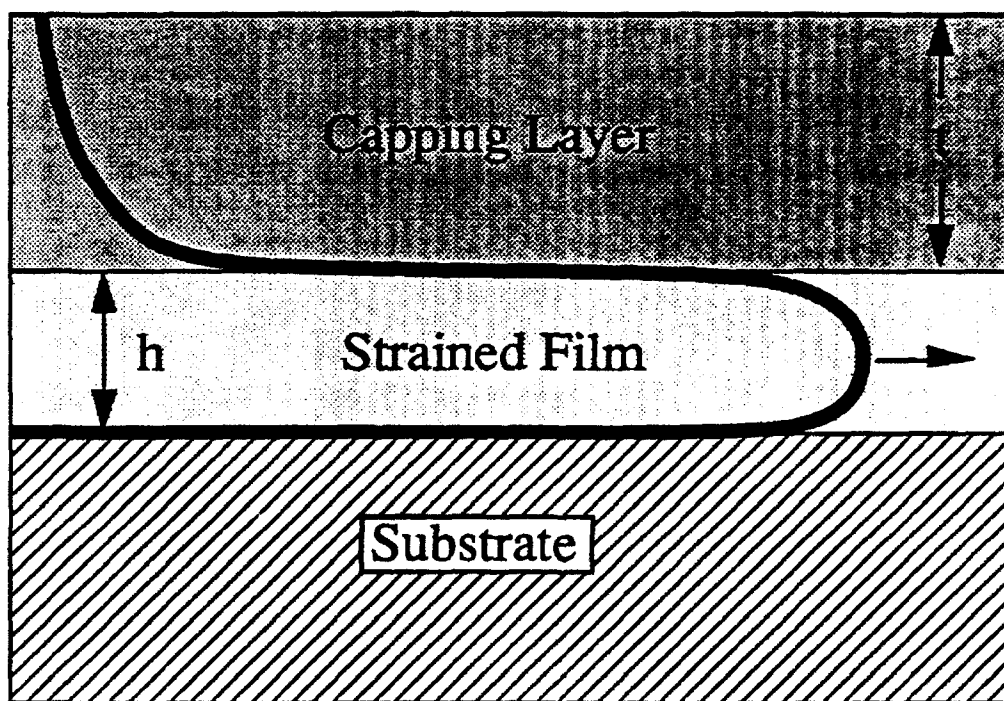
Fig. 8.　Motion of a threading that is confined to remain within the strained film. The capping layer is too thick for the dislocation to cut through. The velocity of the dislocation is v(dipole).

Finally, we consider the rate of motion of a "threading" dislocation that extends from the film/capping layer interface to the free surface of the capping layer, as shown in Fig. 9. The motion of the dislocation segment is not driven by the stress in the film. Rather it is driven by the differences in energy of the misfit dipole and the single misfit dislocation left at the film/substrate interface when the segment in question moves by. For this kind of movement and for the case in which the capping layer is thin compared to the film, the effective shear stress can be expressed as

$$\tau_{eff}^{catch-up} = A\frac{1}{t}\left\{\ln\left(\frac{\sqrt{3}\beta h}{2\sqrt{2}b}\right) + \ln\left(\frac{\beta t}{b}\right) - \ln\left(\frac{\beta(h+t)}{b}\right)\right\} \quad , \tag{18}$$

where the term "catch-up" refers to the fact that the segment in question is attempting to catch-up with the segment that deposits the dipole in its motion. The first two terms in the brackets relate to the energies of the two dislocations in the dipole while the last term relates to the energy of the single dislocation left behind by the moving dislocation segment.
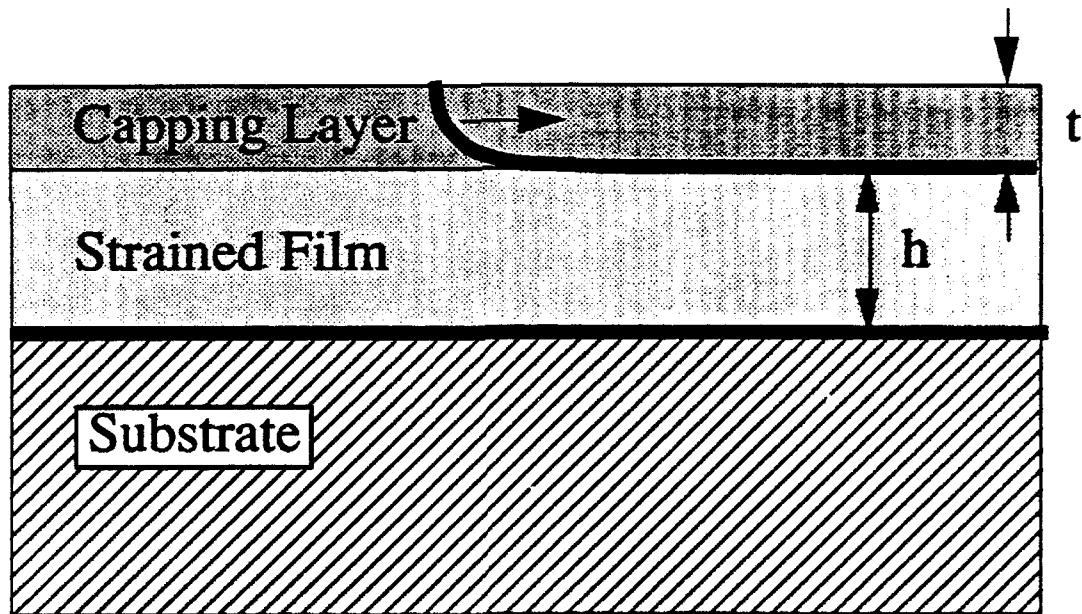
Fig. 9.   Motion of a dislocation segment in the capping layer. The dislocation is moving to catch-up with the leading edge of the dipole not shown in the figure. The velocity of the dislocation is v(catch-up).

Equations (16), (17) and (18) have been used in conjunction with eqn. (10) to examine the influence of capping layers on the velocities of the various dislocation segments under consideration. One set of results is shown in Fig. 10 where the different velocities are shown as a function of capping layer thickness for a 50 nm thick Si-Ge film. The velocities are normalized in

15

such a way that the velocity for an uncapped film is 0.64, as shown by the arrow. Consider first the velocity v(cut) associated with the motion of a "threading" dislocation that cuts through the capping layer. This velocity falls continuously with increasing capping layer thickness. When the capping layer is 3 or 4 times thicker than the film, v(cut) is about an order of magnitude smaller than the velocity for an uncapped film. However, for capping layers of this thickness, the dislocation is not able to move by cutting through the capping layer. Rather the segment that lies in the strained film will move more quickly than the segment that lies in the capping layer, with the result that a dipole configuration is eventually formed. Figure 10 also shows calculated velocities for the dipole configuration. The velocity v(dipole) decreases with increasing capping layer thickness and is smaller than v(cut) up to a critical capping layer thickness of about 35 nm. Beyond that capping layer thickness, v(dipole) is constant because the energy of the dipole does not depend on the thickness of the capping layer. The variation of v(dipole) with capping layer thickness at small capping layer thicknesses is due to the fact that the dipole energy depends on capping layer thickness in that regime. A comparison of v(cut) and v(dipole) indicates that cutting is the dominant process at small capping layer thicknesses, as expected, and that dipole formation dominates at large capping layer thicknesses. The overall result is that the capping layer decreases the dislocation velocity by, at most, a factor of 2.

It is of interest compare the velocity v(catch-up) with v(cut) and v(dipole). Figure 10 shows that below the critical capping layer thickness of 35 nm, v(catch-up) is greater that both v(cut) and v(dipole), whereas at thicknesses greater that the critical thickness, v(catch-up) < v(cut) < v(dipole). This result is understandable and is to be expected. If a dipole configuration existed in a sample with a very thin capping layer, then the segment in the capping layer would quickly catch-up with the leading edge of the dipole and convert the dislocation into a cutting type "threading" dislocation.

A final note should be made about the present analysis. The calculations we have made apply to strained films that have not yet relaxed. In this limit the capping layer is under no biaxial stress. During the course of strain relaxation in films with thin capping layers, the moving dislocations plastically deform both the film and the capping layer. This relieves the strain in the strained layer but it causes a strain of opposite sense to develop in the capping layer. This effect, which was not taken into account in the above analysis, would reduce the critical capping layer thickness for forming the dipole configuration and would slow the speed of cutting type dislocations.
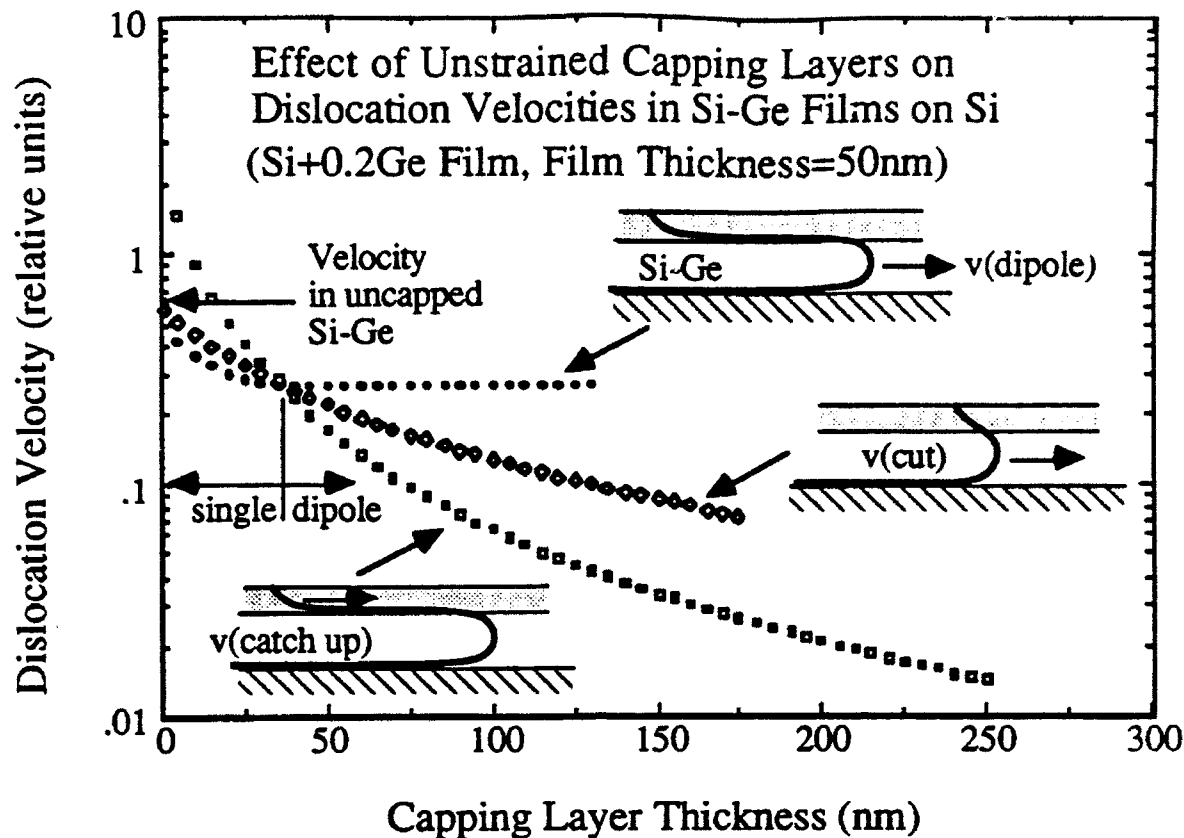
16

Fig. 10   A comparison of various dislocation velocities as a function of capping layer thickness. The critical capping layer thickness above which dislocations move by the dipole process is about 35 nm.

Effects of Unstrained Capping Layers on the Nucleation and Multiplication of "Threading" Dislocations

The analysis described in the previous section indicates that "threading" dislocation velocities are reduced by only as much as a factor of 2. As we shall see, this small effect cannot account for the large inhibiting effects of unstrained capping layers on the formation of misfit dislocations.

A full accounting of the effects of unstrained capping layers must include the effects on nucleation and multiplication of "threading" dislocations. Unstrained Si capping layers of various thicknesses were grown on dislocation free Si-Ge films by the LRP technique. These samples were then annealed at 850°C for 4 minutes, either in a rapid thermal oven outside of the growth chamber (ex-situ) or in the LRP growth chamber prior to removal of the substrate (in-situ). The misfit dislocation spacings in both capped and uncapped films were measured after annealing. The

17
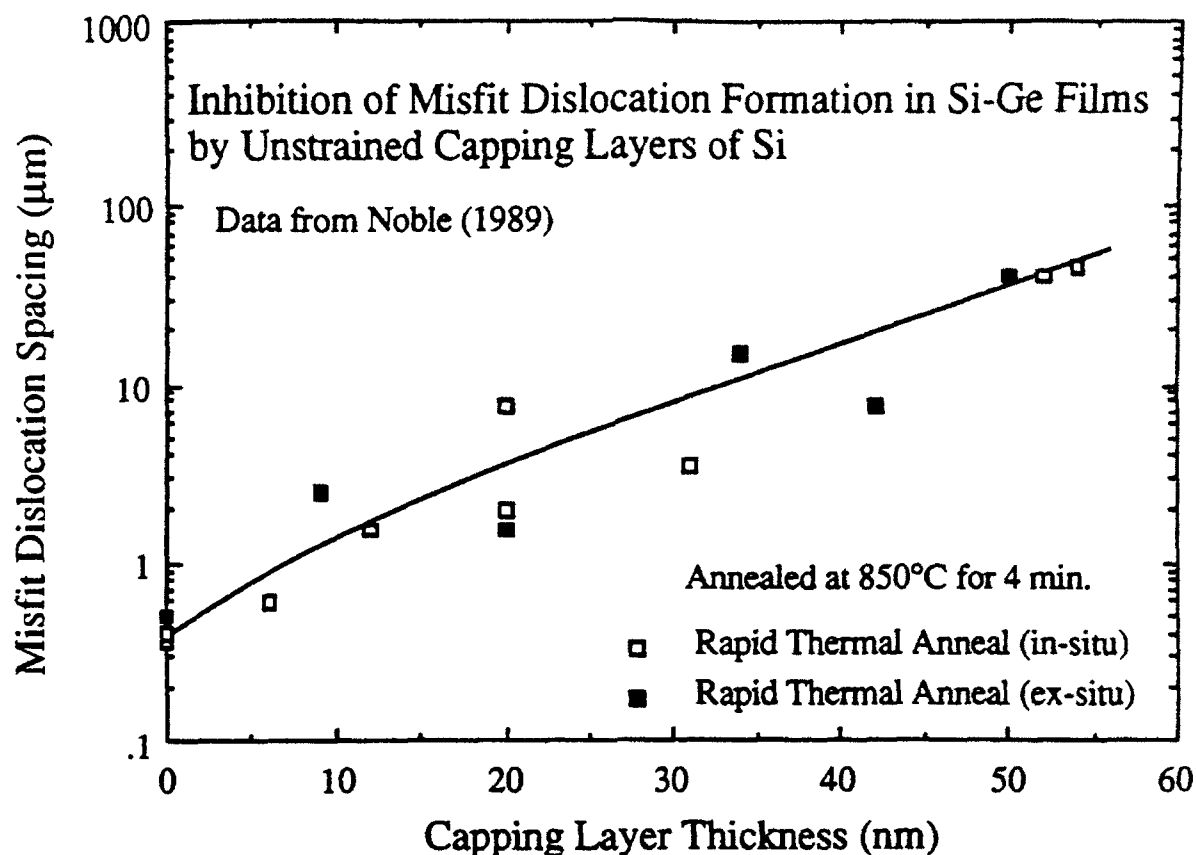
Fig. 11. Effect of capping layer thickness on the misfit dislocation spacing in Si-Ge films after annealing at 850°C for 4 minutes. The capping layers greatly inhibit misfit dislocation formation.

results are shown in Fig. 11. As shown in the figure, the annealing process allows a high density of misfit dislocations to form. The misfit dislocation spacing for the uncapped film is about 0.5 μm. As can be seen in the figure, the misfit dislocation spacing after annealing increases markedly with increasing capping layer thickness. For a capping layer thickness of 50 nm, the misfit dislocation spacing is more than 100 times greater than the misfit dislocation spacing for uncapped films. By comparison, a 50 nm capping layer decreases the "threading" dislocation velocity by only about a factor of 2. This indicates strongly that something other that the "threading" dislocation velocity must be affected by the capping layer. We believe the primary effect of the capping layer is to inhibit misfit dislocation nucleation and multiplication.

18

References

1. M.P. Scott, S.S. Laderman, T.I. Kamins, S.J. Rosner, K. Nauka, D.B. Noble, J.L. Hoyt, C.A. King, C.M. Gronet and J.F. Gibbons, Mater. Res. Soc. Symp. Proc., 130, 179-184 (1989).

2. R. Hull, J.C. Bean and C. Buescher, J. Appl. Phys., 66, 5837-5843 (1989).

3. G.L Patton, J.H. Comfort, B.S. Meyerson, E.F. Grabbe, G.J. Scilla, E. De Fresart, J.M.C. Stork, J.Y.-C. Sun, D.L. Harame and J.M. Burghartz, IEEE Electron Device Letters, 11, 171-173 (1990).

4. T.I. Kamins, K. Nauka, J.B. Kruger, J.L. Hoyt, C.A. King, D.B. Noble, C.M. Gronet and J.F. Gibbons, IEEE Electron Device Letters, 10, 503-505 (1989).

5. D.J. Stirland, Appl. Phys. Letters, 53, 2432-2437 (1988).

6. J.H. Van der Merwe, J. Appl. Phys., 34, 123-127 (1963).

7. J.W. Matthews and A.E. Blakeslee, J. Cryst. Growth, 27, 118-125 (1974).

8. J.W. Matthews and A.E. Blakeslee, J. Cryst. Growth, 29, 273-280 (1975).

9. J.W. Matthews, J. Vac. Sci. Technology, 12, 126-133 (1975).

10. W.D. Nix, Metall. Trans. A, 20A, 2217-2245 (1989).

11. J.C. Bean, L.C. Feldman, A.T. Fiory, S. Nakahara and I.K. Robinson, J. Vac. Sci. Technology A, 2, 436-440 (1984).

12. L.B. Freund, J. Appl. Mech., 54, 553-557 (1987).

13. L.B. Freund, A. Bower and J.C. Ramirez, Mater. Res. Soc. Symp. Proc., 130, 139-152 (1989).

14. B.W. Dodson and J.Y. Tsao, Appl. Phys. Lett., 51, 1325-1327 (1987).

15. J.Y. Tsao, B.W. Dodson, S.T. Picraux and D.M. Cornelison, Phys. Rev. Letters., 59, 2455-2460 (1987).

16. B. Reppich, P. Hassen and B. Ilschner, Acta Metall., 12, 1283-1288 (1964)

17. H. Alexander and P. Hassen, Solid State Physics, 22, 27-158 (1968).

18. R. Hull, J.C. Bean, D.J. Werder and R.E. Leibenguth, Appl. Phys. Lett., 52, 1605-1607 (1988).

19. C.G. Tuppen and C.J. Gibbings, to be published.

20. W. Hagen and H. Strunk, Appl. Phys., 17, 85-87 (1978).

21. M.F. Doerner and W.D. Nix, J. Materials Res., 1, 601-609 (1986).

22. T. Vreeland, Jr., A. Dommann, C.-J. Tsai and M.-A. Nicolet, Mater. Res. Soc. Symp. Proc., 130, 3-12 (1989).

23. P.A. Flinn, D.S. Gardner and W.D. Nix, IEEE Trans. on Electron Devices, ED-34, 689-699 (1987).

24. P.A. Flinn, Mater. Res. Soc. Symp. Proc., 130, 41-52 (1989).

B. In Situ Study of Isothermal Strain Relaxation in Si-Ge Heteroepitaxial Films using Substrate Curvature Measurements

Véronique T. Gillard, David B. Noble* and William D. Nix*

1. Introduction

Lattice mismatch between a heteroepitaxial Si-Ge film and a Si substrate causes elastic misfit strain to exist in the film. When the film thickness is higher than a critical value [1], the biaxial stress associated with this elastic strain can serve as driving force for the movement of threading dislocations. As they move through the film, these threading dislocations lay down misfit dislocations at the film/substrate interface and this causes the elastic strain to relax. Several device applications of Si-Ge heteroepitaxial films are based on the significant reduction of the indirect bandgap caused by the misfit strain [2]. For these applications, relaxation of the misfit strain is not desirable. There exist other applications for which there is a need for a high density of misfit dislocations in conjunction with a low density of threading dislocations [3]. In both cases, understanding of the kinetics of relaxation, as well as the mechanisms involved is important to the development of reliable devices.

The biaxial stress in the film causes elastic bending of the substrate. The resulting substrate curvature is related to the elastic strain in the film through the following equation.

$$\varepsilon = \frac{M_s}{M_f} \frac{h_s^2}{6h_f} \Delta K$$

(1)

where M represents biaxial modulus, h represents thickness and ΔK is the difference in curvature between bare substrate and substrate with film. The subscripts "s" and "f" refer to substrate and film, respectively. During isothermal annealing experiments, the change in substrate curvature with time is measured with a laser scanning system [4]. The relaxation of elastic strain and the corresponding evolution of plastic strain are found using the above formula.

The kinetics of formation of misfit dislocations can be studied by considering that they are deposited at the film/substrate interface by threading dislocations moving through the film. Since each threading dislocation creates a misfit dislocation as it moves, the mean spacing, S, between misfit dislocations varies with time according to the following formula [1].

$$\frac{d\left(\frac{1}{S}\right)}{dt} = \frac{Nv}{2} \qquad (2)$$

In the above equation, v is the threading dislocation velocity, N, the mobile threading dislocation density, and the factor of 2 is related to the 60° misfit dislocations. This equation shows that the kinetics of misfit dislocation formation depends on the threading dislocation velocity and the density of mobile threading dislocations, both of which vary during the course of relaxation. It is necessary to separate these two parameters and their evolution with time in order to better understand the kinetics of relaxation.

The kinetics of movement of the threading dislocations can be studied using an argument which considers that the work done on the moving dislocation by the stress in the film has to be greater than the work necessary for the formation of the misfit dislocation. This method leads to a value for the effective shear stress, which is the stress still available to drive the threading dislocation forward after a misfit dislocation has been deposited in its wake [1]:

$$\tau_{eff} = \tau - 0.95 \sqrt{\frac{2}{3}} \frac{b}{4\pi(1-v)} \frac{2\mu_f \mu_s}{(\mu_f + \mu_s)} \frac{1}{h_f} \ln\left(\frac{\beta \ h_f}{b}\right) \qquad (3) \qquad \tau = \frac{\sigma}{\sqrt{6}} \qquad (3')$$

where b is the Burgers vector of the misfit dislocation, v is Poisson's ratio, μ_s and μ_f are the shear moduli of the substrate and film, respectively, and β is a constant equal to 0.755 [1].
σ is the biaxial stress in the film, τ is the resolved applied shear stress and the expression appearing after the minus sign represents the part of the shear stress which is required for the formation of the misfit dislocation. Since the variation of the elastic strain with time during the annealing experiment is known, the corresponding variation of the resolved shear stress τ is also known and this allows for a determination of the effective shear stress as a function of time using equation (3).

If the rate of motion of threading dislocations is assumed to be governed by the thermally activated nucleation and motion of kinks along the dislocation line, the empirical equation developed by Alexander and Hassen [5] may be used to relate the threading dislocation velocity to the effective stress:

$$v = B \exp\left(\frac{-U}{kT}\right) * \left(\frac{\tau_{eff}}{\tau_0}\right)^n \qquad (4)$$

U is the activation energy for dislocation motion, n, B and τ_0 are constants, τ_{eff} is the effective stress given by equation (3) and the other terms have their usual meaning. In the present study, the activation energy and the constants are determined in films similar to those studied in the annealing experiments using a least square method to fit velocities measured by TEM and effective shear stresses. Since the nucleation and motion of kinks is a near-atomic scale process, the use of equation (4), which was developed for bulk material, is expected to be applicable for thin films [1]. Furthermore, as will be shown later in this paper, this equation gives a good mathematical description of our experimental data.

As mentioned earlier, the formation of misfit dislocations causes the homogeneous elastic strain in the film to relax. The Orowan equation may be used to express the biaxial plastic strain rate in the following manner

$$\dot{\varepsilon} = \frac{1}{4}Nvb \qquad \Rightarrow \qquad N = \frac{4\,\dot{\varepsilon}}{v\,b} \tag{5}$$

Since the variation of the effective shear stress with time during the annealing experiment is known (equation (3)), the corresponding variation of the threading dislocation velocity, v, with time is determined using equation (4). The evolution of the strain rate, $\dot{\varepsilon}$, is also determined from the evolution of strain, ε, as a function of time. Using equation (5) then allows us to obtain the evolution of N, the mobile dislocation density, during the course of annealing.

There are several physical mechanisms which can cause the mobile dislocation density to change during the relaxation process. N can increase if threading dislocations are nucleated and/or if dislocation multiplication is occurring; these phenomena are predominant in the early stage of relaxation when the available driving force is still high. The mobile dislocation density can decrease if threading dislocations are lost at the edge of the film and/or if dislocation interactions cause immobilization. The shape of the curve N(t) is determined by the mechanism(s) causing the mobile dislocation density to change. For example, at the start of the relaxation, the general shape of N(t) depends on whether nucleation or multiplication of dislocation is the dominant process, as shown in Fig. 1.

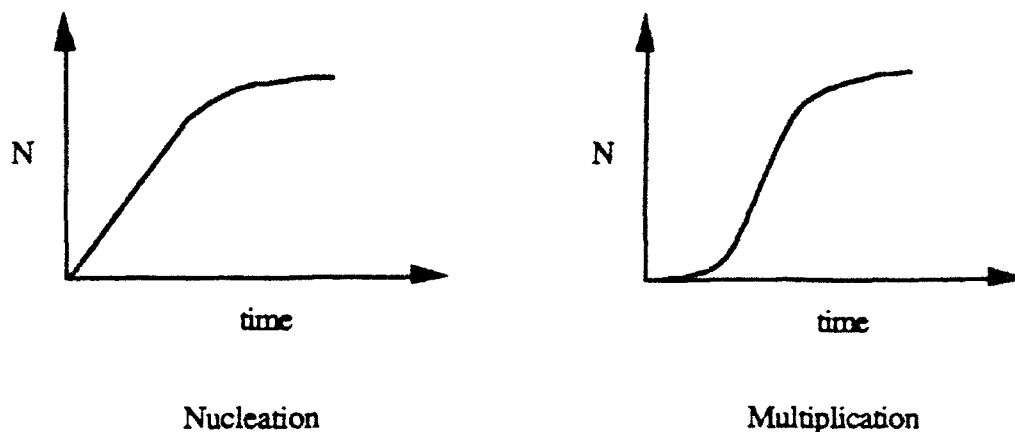Nucleation   Multiplication

Figure 1. General shape of mobile dislocation density versus time with nucleation or
multiplication being the predominant mechanism of dislocation creation.

If nucleation is the dominant process for threading dislocation formation, the mobile dislocation density should start to increase immediately and continue to increase at a fairly constant rate. On the other hand, if multiplication, through a mechanism such as Hagen-Strunk [6], dominates, it will take a certain amount of time before a source is created and N(t) will remain flat until multiplication can start, then, N is expected to increase exponentially with time [1].

$$\left(\frac{dN}{dt}\right)_{multiplication} = N \delta \, v$$

(6)

Here δ is a breeding factor as in the creep literature. The ability to determine the evolution of the mobile dislocation density with time during annealing experiments should therefore help to develop a better understanding of the mechanisms of relaxation.

2.   Sample and Experiment Characteristics

The Si-Ge films were grown in Prof. Gibbons' laboratory at Stanford on (001), heavily n doped, 3" Si wafers. An undoped Si layer was used as a buffer between the Si-Ge film and the doped substrate. The growth was performed at 625 °C in a lamp-heated CVD reactor in the reaction-limited regime. The 6 samples used in this study have a Ge fraction of 34.5% ($\pm$ 0.5%) and film thicknesses of 100, 400, 500, 600, 700, and 800 Å. Both Ge content and film thickness were measured after growth by RBS. The 100 Å film thickness was verified by cross-section TEM.

After growth, a 1 by 1 inch piece was cut from the center of the wafer to ensure film thickness uniformity over the sample. The substrate was then thinned to about 200 µm in order to increase the curvature and thereby improve the strain measurement resolution. TEM observations of the samples showed that all films, except the 100 Å thick film, contain a certain number of misfit dislocations after film growth. The 100 Å film is very near the critical thickness for relaxation.

The elastic strain in the film after growth was determined using a combination of x-ray diffraction and wafer curvature measurements.

An annealing temperature of 700 °C was chosen and the annealing procedure was as follows: a sample was inserted in the furnace previously stabilized at 700 °C in an argon atmosphere and reached the target temperature within 2 minutes. Starting immediately after insertion, substrate curvature was measured in situ every 2 minutes for several hours. Readers should refer to von Preissig, [4] for a detailed description of the furnace and the curvature measurement system.

3.   Experimental Results

A calculation of the misfit strain, ϵ_m, in a Si-Ge film containing 34.5 % Ge, gives a compressive biaxial strain of -1.30 % at room temperature and -1.37 % at 700 °C. These results are based on a film lattice parameter which takes into account the negative deviation from Vegard's law [7]. The misfit strain at 700 °C is determined using experimental data for the variation of the linear expansion coefficient of Si and Ge with temperature [8-9] and a simple rule of mixtures for the linear expansion coefficient of Si-Ge. Using a direct measurement of the Si-Ge lattice parameter at 700 °C for a Ge fraction of 34.7% [7] leads to a value of -1.36 %.

Experimental values for the misfit strain and the elastic strain remaining in the films after growth are presented in Table I.

Measured values of strain are not available for the 100 Å film. One can see in Table I that the experimental value obtained for the misfit strain at room temperature (ϵ_m R.T.) is very close to the calculated value given above (-1.30 %). However, the misfit strain measured at 700 °C, (ϵ_m 700°C) is significantly smaller than that calculated on the basis of lattice parameter measurements published in the literature [7], (-1.36 %). This effect does not seem to be caused by the curvature measurement system, as the change in curvature due to temperature gradients through the substrate thickness has been previously measured [4] and leads to strain variations which are an order of magnitude smaller than those observed here. Furthermore this effect is not observed on a bare Si

24

substrate. Therefore, it seems that as the samples are heated to 700 °C, a small part of the elastic strain is immediately relaxed even in the case of a film which exhibits no further relaxation for about an hour, (400 Å film) as shown later. We are unable to explain this phenomenon at present. Samples similar to those described in this study but grown by MBE show the same type of effect.

Table I
Experimental values of strain [%].

h_f [Å]	$\varepsilon_{el.(1)}$ R.T.	$\varepsilon_{el.(1)}$ 700°C	ε_{pl}	ε_m R.T.	ε_m 700°C
400	-1.26	-1.21	-0.00	-1.26	-1.21
500	-1.25	-1.19	-0.00	-1.25	-1.19
600	-1.25	-1.21	-0.01	-1.26	-1.22
700	-1.28	-1.22	-0.04	-1.32	-1.26
800	-1.12	-1.07	-0.13	-1.25	-1.20

$\varepsilon_{el.(1)}$ R.T. is the remaining elastic strain after growth measured with a combination of x-ray diffraction method and wafer curvature at room temperature.

$\varepsilon_{el.(1)}$ 700°C is the elastic strain measured with the wafer curvature technique immediately after sample insertion in the furnace. Sample temperature is already within 5 °C of the target temperature at the time of measurement.

ε_{pl} is the plastic strain corresponding to the amount of relaxation which took place during growth determined using TEM measurements of average misfit dislocation spacing, S, ($\varepsilon_{pl} = b/2S$).

(ε_m R.T.) = ($\varepsilon_{el.(1)}$ R.T.) + (ε_{pl}) and (ε_m 700°C) = ($\varepsilon_{el.(1)}$ 700°C) + (ε_{pl})

The results of the annealing for the 6 samples are presented in Fig. 2. This figure shows that, as expected, the 100 Å film, which is very near the critical thickness, does not substantially relax. The 400 Å film shows a long plateau with no significant relaxation, then, the elastic strain starts to decrease very rapidly until relaxation decelerates and a new plateau is reached. The 500 Å film behaves in a very similar manner but the relaxation occurs more quickly. This is expected since the

driving force is higher in this thicker film. In the other films, no plateau is observed as strain relaxation had already started during growth.
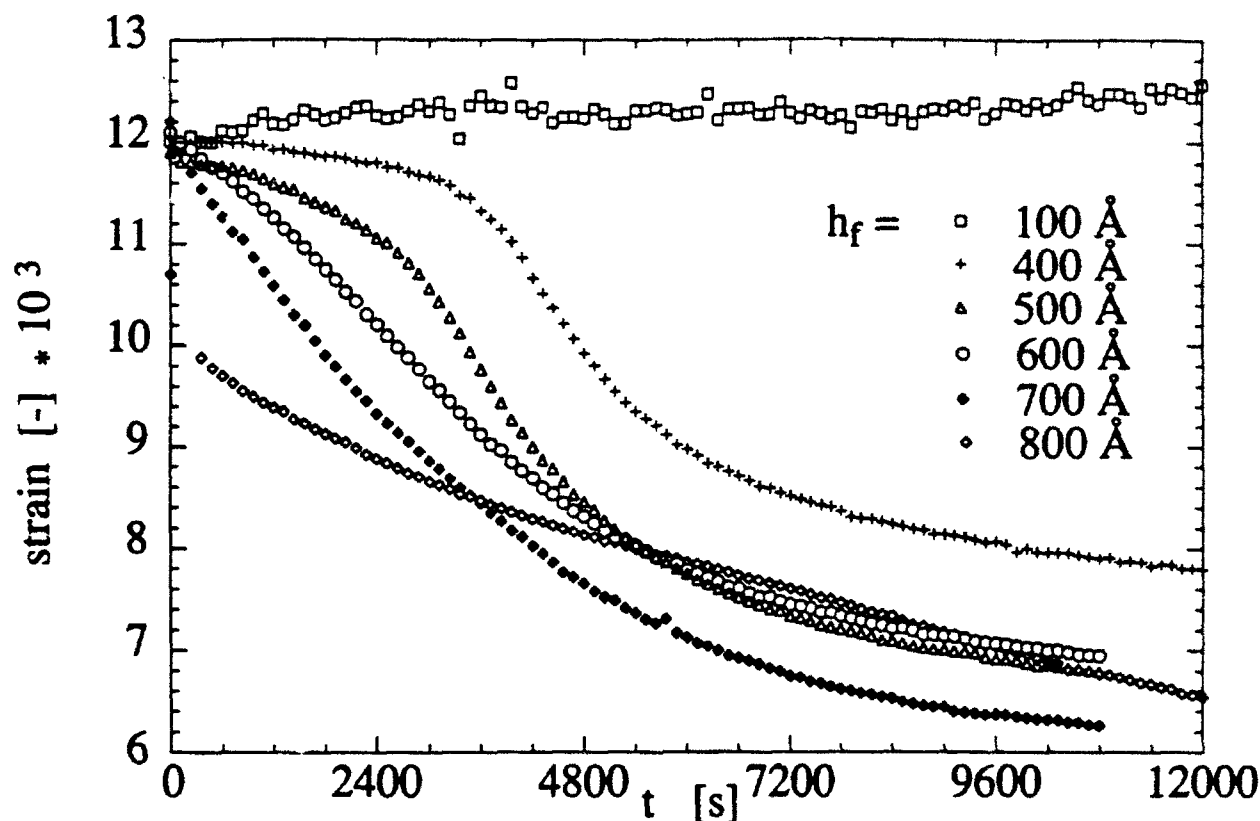

Figure 2. Residual elastic strain versus time during annealing at 700 °C.

In the case of the 800 Å film, most of the relaxation already occurred before annealing and the curve recorded only shows the decelerating part of the strain relaxation. The variation of the shape of the relaxation curves with film thickness is consistent with the fact that the driving force for strain relaxation increases as the film becomes thicker.

Figure 3 shows experimental data of dislocation velocities versus effective stress for bulk material [10] and for thin films (TEM). Both sets of data lie on the same line, which represents the best least square fit to equation (4). This shows that the equation developed by Alexander and Hassen gives a good representation of our velocity data. For the following part of this study, we determine the constants in equation (4) by fitting Noble's data only, since they are measured in films very similar to those studied here, which contain a certain amount of oxygen. We get the

26

following values: the activation energy U is 2.1 eV, the exponent n is 0.86, and the other constants are B = 19300 m/s and τ_0 = 9 8 MPa.
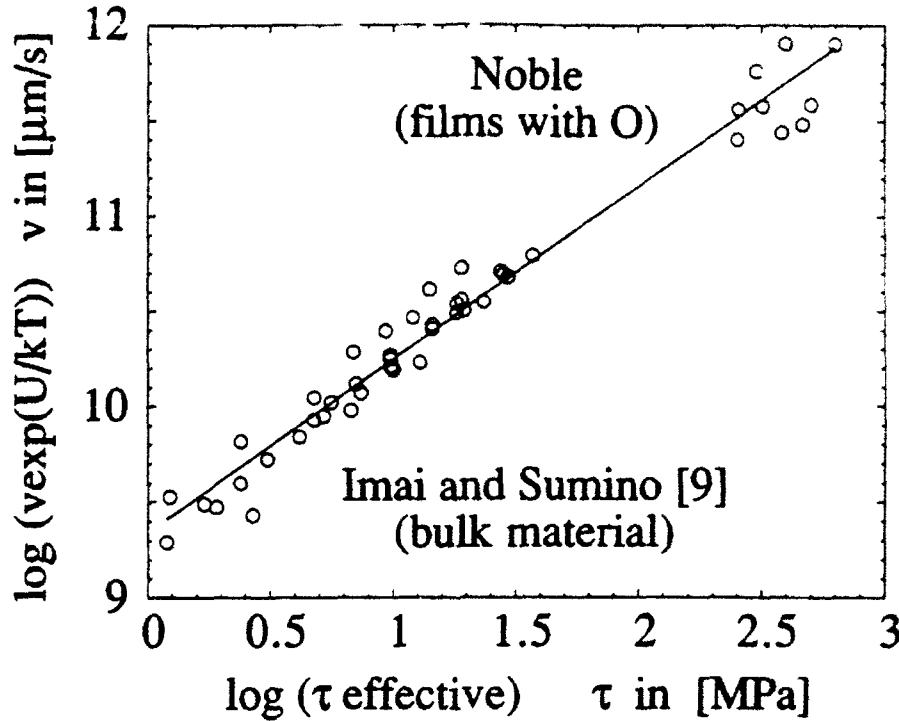

Figure 3. Variation of dislocation velocity with effective stress.

Using the measurement of strain versus time, we determine the variation of strain rate during the course of relaxation. This data is presented in Fig. 4 for the 400 Å thick film. Also presented in this figure is the variation of dislocation velocity with annealing time determined using equation (4) with the values given above for the constants. Then, the mobile dislocation density, N, is determined with equation (5) and leads to the curves displayed in Fig. 5. In this figure, we see that for the thickest film, where most relaxation took place during growth, the mobile dislocation density remained rather constant during annealing. The thinner films show a sharp increase in N until a peak is reached, after which the mobile dislocation density decreases very rapidly to reach a plateau. The shape of the curve at the stage where N increases suggests a multiplication mechanism. The decrease in N should be due to a combination of dislocation annihilation at the film's edges and immobilization due to interaction with other dislocations. Using samples with different areas should allow us to determine which of these mechanisms is dominant.
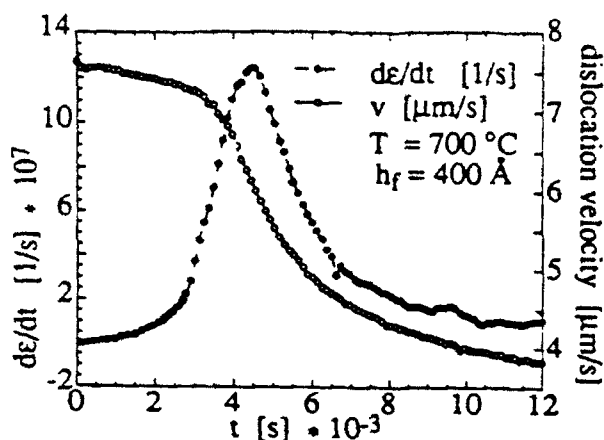
27

Figure 4. Strain rate and dislocation velocity versus time for the 400 Å film.
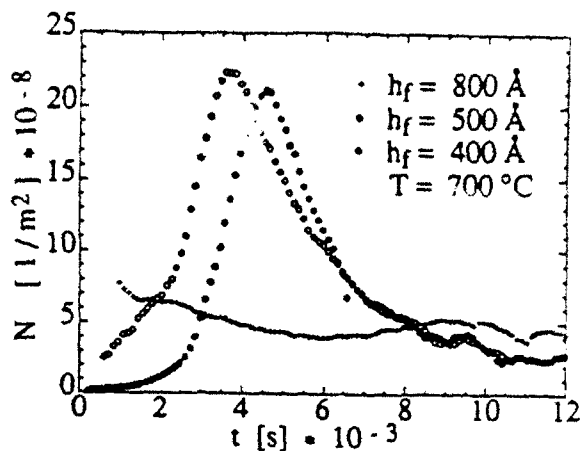
Figure 5. Mobile dislocation density versus time for the 400, 500 and 800 Å films.

4. Conclusions

The combination of curvature measurements taken during annealing experiments and previous TEM dislocation velocity measurements allows us to determine the evolution of mobile threading dislocation density during the course of strain relaxation in Si-Ge films. This should prove to be a useful tool for a better understanding of the kinetics of strain relaxation in heteroepitaxial films and the corresponding mechanisms responsible for that relaxation.

References

1.   W. D. Nix, D. B. Noble, and J. F. Turlo in Thin Films: Stresses and Mechanical Properties II, edited by M. F. Doerner, W. C. Oliver, G. M. Pharr, and F. R. Brotzen (Mater. Res. Soc. Proc. 188, Pittsburgh, PA 1990) pp.315-330.

2.   R. People, Physical Review, B 32, 1405 (1985).

3.   E. A. Fitzgerald, Y.-H. Xie, M. L. Green, D. Brasen, A. R. Kortan, J. Michel, Y.-J. Mii, and B. E. Weir, Appl. Phys. Lett., 59 (7), 811, (1991).

4.   F. J. von Preissig, PhD. Dissertation, Stanford University (1991).

5.   H. Alexander and P.Hassen, Solid State Physics, 22, 27 (1968).

6.   W. Hagen and H. Strunk, Appl. Phys., 17, 85 (1978).

7.   R. Olesinski and G. Abbaschian, Bulletin of Alloy Phase Diagrams, 5 (2), 180 (1984).

8.   Y. Touloukian, R. Kirby, R. Taylor, and P. Desai in Thermophysical Properties of Matter: Metallic Elements and Alloys, (IFI/Plenum, 12, New York, 1975) pp. 116-119.

28

9. Y. Touloukian, R. Kirby, R. Taylor, and T. Lee in <u>Thermophysical Properties of Matter: Nonmetallic Solids.</u> (IFI/Plenum, <u>13</u>, New York, 1977) pp. 154-157.

10. M. Imai and K. Sumino, Phil. Mag., <u>47A</u>, 599 (1983).

III. ORAL PRESENTATIONS RESULTING FROM AFOSR GRANTS NO. 86-0051 AND 86-0051

1. W.D. Nix, "Mechanical Properties of Microelectronic Thin Film Materials", CIS Annual Review, Stanford University, March 6, 1986.

2. W.D. Nix, "New Experimental Techniques for the Study of Mechanical Properties of Microelectronic Thin Files", Department of Mechanical Engineering, University of California, Davis, March 13, 1986.

3. W.D. Nix, Mechanical Properties of Thin Films and Other Fine Scale Structures", Albuquerque Chapter of ASM, Albuquerque, New Mexico, March 19, 1986.

4. M.F. Doerner, "Mechanical Properties of Thin Films Using Nanoindenter Techniques", Materials Science Industrial Affiliates Program, Stanford University, May 28, 1986.

5. M.F. Doerner and W.D. Nix, "Mechanical Properties of Thin Films on Substrates", Micromechanics Research Group, IBM Research Laboratory, San Jose, California, June 27, 1986.

6. W.D. Nix and M.F. Doerner, "Mechanical Properties of Microelectronic Thin Film Materials: Nanoindenter and Wafer Curvature Techniques", Summer Research Group, Materials Science Center, Los Alamos National Laboratory, August 18, 1986.

7. W. D. Nix, "Mechanical Properties of Thin Films", Materials Science Colloquium, Department of Materials Science and Engineering, Stanford University, December 5, 1986.

8. W. D. Nix, "New Experimental Techniques for the Study of Mechanical Properties of Thin Films", Department of Metallurgical Engineering, The Ohio State University, Columbus, Ohio, February 6, 1987.

9. W.D. Nix, "Mechanical Properties of Thin Films", Department of Materials Science, Ecole Polytechnique de Federale Lausanne, Lausanne, Switzerland, April 15, 1987.

10. M.F. Doerner, "Mechanical Properties of Thin Films Using Sub-Micron Indentation Techniques", TMS Fall Meeting, Cincinnati, October 1987.

11. M.F. Doerner, "Stresses and Deformation Processes in Thin Films on Substrates", TMS Annual Meeting, Phoenix, Arizona, January 1988.

12. W.D. Nix, "Mechanical Properties of Thin Films", Intsitute of Metals Lecture, TMS Annual Meeting, Phoenix, Arizona, January 1988.

13. W.D. Nix, "Mechanical Properties of Thin Films and Other Finely Structured Materials", Micrometallurgy 88, TMS Northern California Meeting, Lake Tahoe, California, March 1988.

14. W.D. Nix, "Mechanisms and Kinetics of Misfit Dislocation Formation in Heteroepitaxial Structures", Symposium on Defects and Defect Reduction Processing in Semiconductor Heterostructures, Annual Meeting of the Metallurgical Society, Anaheim, California, February 19, 1990.

15. R. Venkatraman, J.C. Bravman, P.W. Davies, P.A. Flinn, D.B. Fraser and W.D. Nix, "Mechanical Properties and Microstructural Characterization of Al-0.5%Cu Thin Films", Symposium on Metallization for Electronics Applications, Annual Meeting of the Metallurgical Society, Anaheim, California, February 21, 1990.

16. A.I. Sauter and W.D. Nix, "Finite Element Calculations of Thermal Stresses in Passivated and Unpassivated Lines Bonded to Substrates", Symposium on Thin Films: Stresses and Mechanical Properties, Spring Meeting of the Materials Research Society, San Francisco, April 18, 1990.

17. W.D. Nix, D.B. Noble and J.F. Turlo, "Mechanisms and Kinetics of Misfit Dislocation Formation in Heteroepitaxial Structures", Symposium on Thin Films: Stresses and Mechanical Properties, Spring Meeting of the Materials Research Society, San Francisco, April 19, 1990.

18. W.D. Nix, "Mechanical Properties of Thin Films", Special Foreigner's Lecture, Japan Institute of Metals, Tohoku University, Japan, September 24, 1990.

19. W.D. Nix, "Mechanical Properties of Thin Films", 1991 Spring Meeting of the German Physical Society, Munster, Germany, April 9, 1991

20. W.D. Nix and A.I. Sauter, "Modelling Void Growth and Failure of Passivated Metal Lines under Stress and Electromigration Conditions" First International Workshop on Stress Induced Phenomena in Metallizations, Ithaca, New York, September 11-13, 1991.

21. V.T. Gillard and W.D. Nix, "In Situ Study of Isothermal Strain Relaxation in Si-Ge Heteroepitaxial Films using Substrate Curvature Measurements" Symposium on Thin Films: Stresses and Mechanical Properties III, Fall Meeting of the Materials Research Society, Boston, MA, December 2-6, 1991.

22. W.D. Nix, "Mechanical Properties of Thin Films", Symposium X, Spring Meeting of the Materials Research Society, San Francisco, CA, April 27 - May 1, 1992.

IV. PUBLICATIONS RESULTING FROM AFOSR GRANTS NO. 89-0185 AND 86-0051

1. D.-B. Kao, J.P. McVittie, W.D. Nix and K.C. Saraswat, "Two-Dimensional Oxidation: Experiments and Theory", Proceedings of IEDM 85, IEEE, 1985, p. 388.
   (selected as best student paper at the conference)

2. M.F. Doerner and W.D. Nix, "A Method for Interpreting the Data from Depth-Sensing Indentation Instruments", J. Materials Research, 1, 601 (1986).

3. M.F. Doerner, D.S. Gardner and W.D. Nix, "Plastic Properties of Thin Films on Substrates as Measured by Submicron Indentation Hardness and Substrate Curvature Techniques", J. Materials Research, 1, 845 (1986).

4. P.A. Flinn, D.S. Gardner and W.D. Nix, "Measurement and Interpretation of Stress in Aluminum-Based Metallization as a Function of Thermal History", IEEE Trans. on Electron Devices, ED-34, 689 (1987).

5. D.-B. Kao, J.P. McVittie, W.D. Nix and K.C. Saraswat, "Two-Dimensional Thermal Oxidation of Silicon - I. Experiments", IEEE Trans. on Electron Devices, ED-34, 1008 (1987).

6. D.-B. Kao, J.P. McVittie, W.D. Nix and K.C. Saraswat, "Two-Dimensional Thermal Oxidation of Silicon - II. Modelling Stress Effects in Wet Oxides", IEEE Trans. on Electron Devices, ED-35, 25 (1988).

7. M.L. Ovecoglu, M.F. Doerner and W.D. Nix, "Elastic Interactions of Screw Dislocations in Thin Films on Substrates", Acta Metall., 35, 2947 (1987).

8. M.F. Doerner and W.D. Nix, "Stresses and Deformation Processes in Thin Films on Substrates", CRC Critical Reviews of Solid State and Materials Sciences, 14, 225 (1988).

9. M.F. Doerner and S. Brennan, "Strain Distribution in Thin Aluminum Films using X-Ray Depth Profiling", J. Appl. Phys., 63, 126 (1988).

10. J.C. Bravman, W.D. Nix, D.M. Barnett and D.A. Smith (Editors), "Thin Films: Stresses and Mechanical Properties", Materials research Symposium Proceedings, 130, (1989).

11. F.J. von Preissig, "Applicability of the Classical Curvature-Stress Relation for tThin Films on Plate Substrates", J. Appl. Phys., 66, 4262 (1989).

12. W.D. Nix, "Mechanical Properties of Thin Films", Metall. Trans. A, 20A, 2217 (1989).

13. A.I. Sauter and W.D. Nix, "Finite Element Calculations of Thermal Stresses in Passivated and Unpassivated Lines Bonded to Substrates", Materials Research Symposium Proceedings, 188, 15-20 (1990).

14. W.D. Nix, D.B. Noble and J.F. Turlo, "Mechanisms and Kinetics of Misfit Dislocation Formation in Heteroepitaxial Thin Films", Materials Research Symposium Proceedings, 188, 315-330 (1990).

15. E.Arzt and W.D. Nix, "A Model for the Effect of Line Width and Mechanical Strength on Electromigration Failure of Interconnects with "Near-Bamboo" Grain Structures", Journal of Materials Research, 6, 731-736 (1991).

16. B. Greenebaum, A.I. Sauter, P.A. Flinn and W.D. Nix, "Stress in Metal Lines Under Passivation: Comparison of Experiment with Finite Element Calculations", Appl. Phys. Letters, 58, 1845-1847 (1991).

17. D.B. Noble, J.L. Hoyt, W.D. Nix, J. F. Gibbons, S.S. Laderman, J.E. Turner and M.P. Scott, "The Effect of Oxygen on the Thermal Stability of $Si_{1-x}Ge_x$ Strained Layers", Appl. Phys. Letters, 58, 1536-1538 (1991).

18. W.D. Nix and E. Arzt, "On Void Nucleation and Growth in Metal Interconnect Lines under Electromigation Conditions", Metall. Trans. A, 23A, 2007-2013 (1992).

19. A.I. Sauter and W.D. Nix, "A Study of Stress-Driven Diffusive Growth of Voids in Encapsulated Interconnect Lines", Journal of Materials Research, 7, 1133-1143 (1992).

20. W.D. Nix and A.I. Sauter, "Modelling Void Growth and Failure of Passivated Metal Lines under Stress and Electromigration Conditions", Proceedings of the First International Workshop on Stress Induced Phenomena in Metallizations, American Vacuum Society, Series 13, American Institute of Physics, Conference Proceedings No. 263, 89-104 (1992).

21. F.J. von Preissig and W.D. Nix, "Application of Stress Measurement to the Study of Thermally Activated Processes in Thin-Film Materials", Materials Research Symposium Proceedings, 239, 207-212 (1992).

22. V.T. Gillard, D.B. Noble and W.D. Nix, "In Situ Study of Isothermal Strain Relaxation in Si-Ge Heteroepitaxial Films using Substrate Curvature Measurements", Materials Research Symposium Proceedings, 239, 395-400 (1992).

23. E. Arzt, O. Kraft, J. Sanchez, S. Bader and W.D. Nix, "Electromigration Resistance and Mechanical Strength: New Perspectives for Imterconnect Materials", Materials Research Symposium Proceedings, 239, 677-682 (1992).

Edited Volume:

1. W.D. Nix, J.C. Bravman, E. Arzt and L.B. Freund (Eds.), Thin Films: Stresses and Mechanical Properties III, Materials Research Society Pittsburgh, PA (1992).